

Volatile organic compound emissions from Scots pine: Mechanisms and description by algorithms

Min Shao,¹ Kristin V. Czapiewski,^{2,3} Arnd C. Heiden,^{2,4} Klaus Kobel,²
Michael Komenda,⁵ Ralf Koppmann,⁵ and Jürgen Wildt²

Abstract. The mechanisms of volatile organic compound (VOC) emissions from Scots pine (*Pinus sylvestris* L.) were investigated in laboratory experiments. The plants emitted mainly monoterpenes and acetone. Isoprene was emitted only in small amounts, but the mechanisms of its emissions were similar to those of the other compounds. Isoprene, acetone, and monoterpene emissions from Scots pine could be well described by an algorithm that considers emissions caused by evaporation of VOCs out of pools and emissions in parallel with their biosynthetic production. Monoterpene emissions were mainly affected by temperature. In some cases, monoterpene emissions were also influenced by photosynthetic active radiation implying that monoterpene emissions from *Pinus sylvestris* occur from storage pools as well as from processes that are linked to monoterpene biosynthesis. The coupling of monoterpene emissions with photosynthesis was confirmed by results of experiments with ¹³CO₂. The ¹³CO₂ exposure resulted in emission of ¹³C labeled monoterpenes during ¹³CO₂ exposure as well as during the night following the exposure. Similar results were also obtained for isoprene emissions. Scots pine emitted isoprene during illumination as well as in darkness. The emitted isoprene was labeled during ¹³CO₂ exposure and in the night following the exposure. The results obtained for monoterpene emissions in the laboratory were compared to those of outdoor measurements with Scots pine. While the temperature dependencies of emission rates were comparable to those obtained from laboratory experiments, a PAR dependence was not detectable. Temperature variations during outdoor measurements prevented a detection of this dependence.

1. Introduction

It has been established that monoterpenes are emitted from conifers due to evaporation of these compounds out of resin ducts in the needles. Models describing these emissions consider only physical processes [e.g., Tingley *et al.*, 1991]. Hence emissions from storage pools should be temperature-dependent, but not directly influenced by photosynthetic active radiation (PAR) [Rasmussen, 1972; Dement *et al.*, 1975; Tingley *et al.*, 1980; Lamb *et al.*, 1985; Juuti *et al.*, 1990; Goldan *et al.*, 1995]. On the basis of this model, algorithms have been established to describe monoterpene emissions [Tingley *et al.*, 1991; Lerdau, 1991; Guenther *et al.*, 1993]. Such algorithms are widely used to estimate monoterpene emissions on regional or global scales [Lamb *et al.*, 1987; Simpson *et al.*, 1995; Guenther *et al.*, 1995; Street *et al.*, 1996; Simpson *et al.*, 1999].

However, not all experimental results can be explained by such a simple model. Schuermann *et al.* [1993] observed a

labeling of α -pinene emitted from Norway Spruce (*Picea abies* L. Karst.) with ¹³C atoms only 4 hours after they exposed the plant to ¹³CO₂. They concluded that a substantial part of the emitted monoterpenes must have been synthesized from the CO₂ taken up recently by the plant. Since photosynthesis is related to PAR, a PAR dependence of volatile organic compound (VOC) emission rates can be expected for such a mechanism. Indeed, a PAR dependence of monoterpene emissions has been reported for *Pinus sylvestris* by Janson [1993] and for *Pinus pinaster* by Simon *et al.* [1994].

The PAR dependence of isoprene emissions is well established. Guenther *et al.* [1993] developed an algorithm to describe the temperature and PAR dependence of isoprene emission rates. This algorithm is compatible with a direct coupling between isoprene emission and biosynthesis [Loreto and Sharkey, 1993]. One of the characteristics of this algorithm is that nighttime emission rates are zero.

We observed isoprene emissions from Scots pine during darkness. This indicates that the algorithm of Guenther *et al.* [1993] is not suitable to describe these emissions completely. Furthermore, we found a PAR dependence of the α -pinene and camphene emissions from Scots pine. This behavior cannot be described by the model of Tingley *et al.* [1991]. A combination of these algorithms is required to fully describe the VOC emissions from Scots pine.

We use the emission algorithm suggested by Schuh *et al.* [1997]. This algorithm includes the previously published algorithms of Tingley *et al.* [1991] and Guenther *et al.* [1993] as special cases. It allows to describe a PAR dependence of VOC emission rates as well as nonzero emission rates during dark-

¹State Key Laboratory of Environmental Simulation and Pollution Control, Peking University, Beijing, China.

²Institut für Chemie der Belasteten Atmosphäre, Forschungszentrum Jülich, Jülich, Germany.

³Now at Center for Atmospheric Chemistry, York University, Toronto, Ontario, Canada.

⁴Now at Gerstel GmbH & Co. KG, Mülheim/Ruhr, Germany.

⁵Institut für Chemie und Dynamik der Geosphäre II: Troposphäre, Forschungszentrum Jülich, Jülich, Germany.

ness. It is based on the concept that two independent processes determine VOC emission rates: emissions from storage pools, $\Phi_{\text{VOC}}^{\text{P}}$, and emissions directly coupled to VOC biosynthesis, $\Phi_{\text{VOC}}^{\text{B}}$. Assuming that these two processes are independent, the total emission rate Φ_{VOC} can be calculated from the sum of the individual emission rates:

$$\Phi_{\text{VOC}} = \Phi_{\text{VOC}}^{\text{P}} + \Phi_{\text{VOC}}^{\text{B}}, \quad (1)$$

where $\Phi_{\text{VOC}}^{\text{P}}$ is used to describe emissions due to an evaporation process that only depends on temperature:

$$\Phi_{\text{VOC}}^{\text{P}} = \Phi_{\text{VOC}}^{\text{P},S} \exp \left[\frac{c_{TP}}{R} \left(\frac{T - T_S}{TT_S} \right) \right], \quad (2)$$

where $\Phi_{\text{VOC}}^{\text{P},S}$ is the standard emission rate at standard temperature T_S (usually 25° or 30°C) and zero PAR, R is the gas constant, T is the leaf temperature, and c_{TP} is an empirical parameter mainly determined by the enthalpy of evaporation of an individual compound.

For the emissions directly coupled to VOC biosynthesis the algorithm considers a temperature as well as a PAR dependence similar to the algorithm developed by *Guenther et al.* [1993]. *Schuh et al.* [1997] used the square of the term describing the PAR dependence in the algorithm of *Guenther et al.* [1993] which allows a better description of the PAR dependence they observed for VOC emissions from sunflower. The resulting equation for the emissions coupled to VOC synthesis has the following form:

$$\Phi_{\text{VOC}}^{\text{B}} = \Phi_{\text{VOC}}^{\text{B},S} c_L \left(\frac{\alpha L}{\sqrt{1 + \alpha^2 L^2}} \right)^2 \frac{\exp \left[\frac{c_{T1}}{R} \left(\frac{T - T_S}{TT_S} \right) \right]}{1 + \exp \left[\frac{c_{T2}}{R} \left(\frac{T - T_M}{TT_S} \right) \right]}. \quad (3)$$

In (3), $\Phi_{\text{VOC}}^{\text{B},S}$ is the standard emission rate for the light-dependent emissions at standard light intensity L_S (L_S usually 1000 $\mu\text{mol m}^{-2} \text{s}^{-1}$) and standard temperature. The term c_L is a normalization factor, and α is the parameter that determines the PAR dependence. L is identical to PAR. The temperature dependence of $\Phi_{\text{VOC}}^{\text{B}}$ is determined by the empirical constant c_{T1} . Above the temperature of maximum enzyme activity, T_M , the emission rates decrease with temperature which is described by the denominator including c_{T2} as an empirical parameter.

The algorithm given by *Schuh et al.* [1997] considers VOC emissions in parallel with VOC biosynthesis and emissions from storage pools. No other mechanisms are known so far, and therefore the algorithm should be generally applicable to describe temperature and PAR dependence of VOC emissions. We applied this algorithm to describe the temperature and PAR dependence of the acetone, isoprene, and monoterpene emission rates from Scots pine.

2. Experiment

2.1. Laboratory Experiments

Laboratory studies with *Pinus sylvestris* L. were conducted in continuously stirred tank reactors (CSTR) as described by *Wildt et al.* [1997]. The glass chambers (volume 160, 1000, and 1500 L, respectively) were mounted in temperature-controlled housings. Twelve discharge lamps (Osram HQI 400 W/D) were used for illumination. Filters (OptoChem, type IR3) that re-

flect wavelengths between 750 and 1050 nm were placed between lamps and plant chambers to reduce radiative heating of the plants inside the chambers. At full illumination, PAR at mid canopy height was 360 $\mu\text{mol m}^{-2} \text{s}^{-1}$ (1500 L chamber), 480 $\mu\text{mol m}^{-2} \text{s}^{-1}$ (1000 L chamber), and 800 $\mu\text{mol m}^{-2} \text{s}^{-1}$ (160 L chamber), respectively. The setup allowed varying temperature and PAR independent of each other. The chambers were equipped with several temperature and light intensity sensors as well as air inlet, outlet, and sampling lines. All sampling lines were made either of Teflon (PFA or PTFE) or glass.

Hydrocarbons, ozone, NO, and NO₂ were removed from the inflowing air by a commercial adsorption dryer (Zander, KEA 70) and a palladium catalyst at 450°C. Measurements demonstrated that the concentrations of the studied compounds at chamber inlet were below the detection limit. The flow rate through the chambers (between 20 and 200 L min⁻¹) was controlled by mass flow controllers. Teflon (PTFE) fans inside the chambers ensured rapid mixing of the air.

Mixing ratios of CO₂ and H₂O were measured as described by *Wildt et al.* [1997]. VOC mixing ratios were measured online using two different systems. In most cases, measurements were conducted by gas chromatography in combination with flame ionization detection (GC-FID, Airmotec HC 1010, column: DB-5, 9 m × 0.22 mm ID, film thickness: 1 μm). The setup of the instrument is described in detail by *Schuh et al.* [1997]. In one case a gas chromatography-mass spectrometer system (GC-MSD-system HP5890 Series II-HP5972A, column: SGE BPX-5, 50 m × 0.22 mm ID, film thickness: 1 μm) was used. The setup of this system is described in detail by *Heiden et al.* [1999]. Duration of one measurement was 0.5 hours for the GC-FID system and 1 hour for the GC-MS system; plate numbers were 2.2×10^6 for the GC-MS system and 3.1×10^5 for the GC-FID system, respectively.

2.2. Enclosure Studies

Outdoor measurements with *Pinus sylvestris* L. were conducted using a flow-through enclosure with a volume of approximately 30 L. The experiment was designed to keep temperature and PAR inside the enclosure as close to ambient as possible. During each experiment a single plant was placed inside the enclosure chamber for several days. Air temperature, relative humidity, and PAR were measured inside the enclosure with an HTR-1 probe (PP Systems) at intervals of 5 min. Air was pumped through the enclosure at constant rates of 5–10 L min⁻¹. VOCs were removed from the inlet air by passing it over a Pd/Al₂O₃ catalyst at 450°C. Furthermore, the humidity of the inlet air was reduced to avoid water condensation inside the enclosure. Carbon dioxide was added to the inlet airstream at a rate that allowed to maintain ambient CO₂ concentrations inside the enclosure. For VOC analysis a small fraction (100 mL min⁻¹) of the outflowing air was sampled on a glass tube (180 mm long, 4 mm ID) containing Tenax TA and Carbotrap and analyzed with a GC-MS system. A detailed description of the enclosure system is given by *Komenda et al.* [2001]; the analytical system is described by *Wedel et al.* [1998].

2.3. Identification and Calibration

For both GC-MS systems, identification was based on mass spectra and retention times determined by analyzing synthetic samples prepared by dilution of pure chemicals (Fluka and Aldrich, purity >93%) with air. For the GC-FID system, identification was based on the retention times of the individual

compounds as well as on comparison of chromatograms to those taken simultaneously with the GC-MS system. All GC systems were calibrated with permeation or diffusion sources as described by Schuh *et al.* [1997], Gautrois and Koppmann [1999], and Komenda *et al.* [2001].

3. Material and Methods

Pine seedlings were taken from the Hartheimer Wald, a forest area in the Rhine valley near Freiburg, southern Germany. In autumn, 3- to 4-year-old pine seedlings were dug out with the soil surrounding the roots and placed in pots. During the following winter the plants were stored outdoors. Four of the plants were placed in the 1500 L chamber. These plants were investigated for several months. For a $^{13}\text{CO}_2$ labeling experiment a separate pine plant was placed in the 160 L chamber. During storage and during the experiments the soil was wetted with water containing about 700 μM nitrate. Soil humidity was kept between 75 and 85%. Another set of the plants was used for the outdoor enclosure experiments. During these experiments, temperature, PAR, and soil humidity were determined by the ambient conditions.

The needle area of the investigated plants was determined as follows. The number of needles from 10 different branches of outdoor plants was counted to be 135 ± 10 (1σ) per 10 cm branch length for the parts of branches with green needles. A projection of the needles on paper was made with a photocopier, and the projected needle area was determined by scanning the projection and subsequent counting of number of dark pixels. It should be noted that we use the projected needle areas and not the total needle area, which is about 2.5 times larger than the projected area [Peterer and Körner, 1990].

After the measurements, the needles were dried (oven temperature: 45°C, 5 days) and weighed. Needle dry weight was compared to the projected needle area. To convert the numbers given here in units of $\text{mol cm}^{-2} \text{s}^{-1}$ to emission rates in units of $\mu\text{g g(dw)}^{-1} \text{h}^{-1}$, the factor $1.4 \times 10^7 Mw [\mu\text{g g(dw)}^{-1} \text{h}^{-1} / \text{mol cm}^{-2} \text{s}^{-1}]$ can be used where Mw is the molar weight of the respective compound.

All data given here refer to needle temperatures which were measured by microthermistors. Control experiments using infrared imaging showed that the temperature of other needles deviated up to $\pm 1.5^\circ\text{C}$ from the temperature of those needles where the temperatures were measured with the microthermistors. However, these differences were not influenced by changes of chamber temperature or PAR. Therefore the temperatures measured with microthermistors could be used as mean needle temperatures.

The temperature dependence of the emission rates was studied at constant PAR by changing the chamber temperatures in increments of about 5° . Three to five measurements of VOC concentrations were conducted when the needle temperatures were constant.

To study the PAR dependence of emission rates, light intensity was varied stepwise by varying the number of lamps that were turned on. Because of the resulting change in radiative heating, variations of light intensity caused changes in needle temperature. In order to compensate this effect, the chamber temperature was modified until the leaf temperature was within 1°C of the desired value.

Emission rates Φ_{VOC} were calculated from the measured concentrations of the individual VOCs using

$$\Phi_{\text{VOC}} = F/A[\text{VOC}], \quad (4)$$

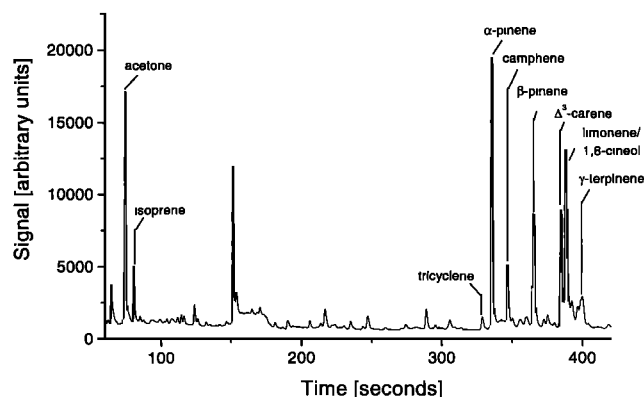


Figure 1. Example of a chromatogram taken from the air at chamber outlet with the GC-FID system. The peak at the retention time of 150 s is an artifact.

where F is the airflow (in unit of mol s^{-1}), A is the leaf area (in units of cm^2), and $[\text{VOC}]$ is the mixing ratio measured for the individual VOC at chamber outlet. It is justified to use (4) because VOC concentrations in the inflowing air were generally below the detection limit and wall losses were negligible for all VOCs except for acetone. Wall losses for acetone varied in the range from below 10% up to 20% of the acetone concentrations that were added to the empty chamber. It was impossible to obtain an exact value for the wall loss, and these losses were neglected. Thus the acetone emission rates given here have to be considered as lower limits.

4. Results

4.1. VOC Emissions

Scots pine emitted mainly acetone, monoterpenes, and sesquiterpenes. Generally, acetone and α -pinene were the most abundant VOCs. A typical chromatogram taken with the GC-FID system is shown in Figure 1. Isoprene emissions from Scots pine were by far lower than those of monoterpenes or those from herbaceous plant species. We used the isoprene emissions to check its emission mechanisms in comparison to those of monoterpenes.

The peaks of limonene and 1,8-cineol overlapped, and no sesquiterpenes were detected in the chromatograms taken with the GC-FID system. Therefore no emission rates could be determined for limonene, 1,8-cineol, and sesquiterpenes for those experiments where measurements were made with the GC-FID system. The GC-MS system was not optimized for concentration measurements of acetone. Data for acetone are from measurements made with the GC-FID system.

4.2. Temperature Dependence

As expected, the emission rates increased with temperature. Figure 2 shows an example for a plot of $\ln(\Phi_{\text{camphene}})$ versus $1/T$. For clarification, the data points taken in darkness and under illumination, respectively, are indicated by different symbols. There was a shift between the data measured during darkness and under illumination, pointing to a PAR dependence of the camphene emission. For the laboratory experiments the temperature dependence of the emissions was determined separately for different levels of PAR. Table 1 shows examples for acetone, isoprene, and the monoterpenes ob-

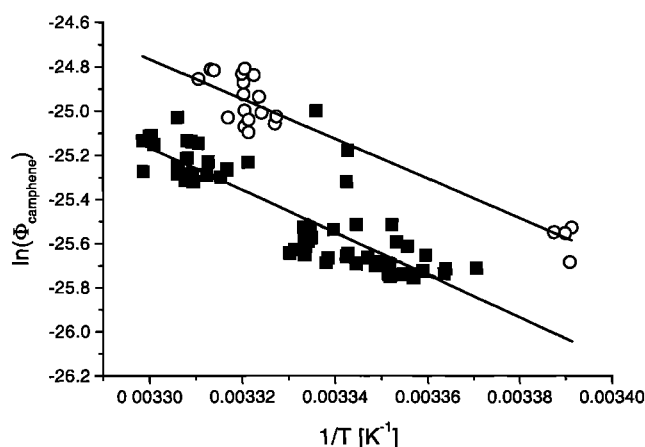


Figure 2. Plot of $\ln(\Phi_{\text{camphene}})$ versus inverse temperature. Open circles: data taken at $\text{PAR} = 360 \mu\text{mol m}^{-2} \text{s}^{-1}$, slope: $9203 \pm 678 [\text{K}^{-1}]$. Solid squares: data taken in darkness, slope: $9534 \pm 805 [\text{K}^{-1}]$. Data from laboratory measurements.

tained from measurements in darkness and at PAR equal to $360 \mu\text{mol m}^{-2} \text{s}^{-1}$.

Three series of measurements regarding the temperature dependence of the emission rates were conducted within a time period of 2 months. Within the error of the measurements, no significant differences were found for the temperature dependencies determined from the different experiments.

Following the model of *Schuh et al.* [1997], VOC emissions in darkness occur from pools. Hence the temperature dependencies given in Table 1 for PAR equal to 0 are the values for c_{TP}/R (equation (2)). During illumination, VOC emissions occur from pools as well as from processes directly related to VOC biosynthesis. During illumination the temperature dependence of the emission rates can be determined by both processes.

To determine the temperature dependence of Φ_{VOC}^B , the following procedure was conducted. The emission rates measured in darkness were normalized to 25°C using (2) and c_{TP}/R as determined from the data measured in darkness. The mean of these normalized emission rates was taken to be $\Phi_{\text{VOC}}^{F,25}$. Thereafter, Φ_{VOC}^B was calculated for those temperatures where the measurements under illumination were performed. Φ_{VOC}^B was obtained by subtracting Φ_{VOC}^F from Φ_{VOC} (compare equation (1)). Linear regression analysis of $\ln(\Phi_{\text{VOC}}^B)$ versus $1/T$ led to the results for c_{T1} .

Reliable results for c_{T1} were obtained only in those cases where the difference $\Phi_{\text{VOC}} - \Phi_{\text{VOC}}^F$ was significant. This was found for the emission rates of acetone, isoprene, α -pinene, and camphene. For β -pinene and Δ^3 -carene it was impossible to find reliable values for c_{T1} . Table 2 shows examples for the results.

Table 2. Temperature Dependence of $\Phi_{\text{VOC}}^B c_{T1}/R^a$

| Acetone | Isoprene | α -pinene | Camphene | T Range, $^\circ\text{C}$ |
|-------------------------|-------------------------|------------------------|-------------------------|-----------------------------|
| 9.2 ± 0.9 (0.86) | 9.0 ± 1.3 (0.74) | 11.4 ± 3 (0.43) | 7.9 ± 2.0 (0.47) | 23–30 |

^aGiven in $[\text{K}] \times 10^{-3} \pm$ standard deviation (1σ), R^2 in brackets. Data obtained after subtracting Φ_{VOC}^F from Φ_{VOC} as measured at $\text{PAR} = 180 [\mu\text{mol m}^{-2} \text{s}^{-1}]$.

Temperature dependencies of monoterpene emissions determined from outdoor measurements were similar to those measured in the laboratory. The data from the outdoor experiments showed a high variability caused by temperature variations during sampling. Owing to the relation between temperature and PAR at ambient conditions, it was impossible to determine temperature dependencies separately for different levels of PAR. Table 3 lists the temperature dependencies measured for the total emission rate Φ_{VOC} for four individual plants.

4.3. PAR Dependence

The emissions of acetone and isoprene were significantly influenced by PAR. For monoterpene emissions, different results were obtained. A low PAR dependence was observed for the α -pinene and camphene emissions. For β -pinene and Δ^3 -carene emissions a PAR dependence was not detectable within the error of measurements.

The data obtained with respect to the PAR dependence were fitted using the algorithm of *Schuh et al.* [1997]. In a first step the fits were conducted for data measured at different levels of PAR but at constant temperature. Φ_{VOC}^F was determined as described above. Then, Φ_{VOC}^F was subtracted from Φ_{VOC} to obtain Φ_{VOC}^B at different levels of PAR. Φ_{VOC}^B determined for PAR equal to $360 \mu\text{mol m}^{-2} \text{s}^{-1}$ ($\Phi_{\text{VOC}}^{B,360}$) was used as the reference, and the data were fitted to

$$\Phi_{\text{VOC}}^B = \Phi_{\text{VOC}}^{B,360} c_L \left(\frac{\alpha L}{\sqrt{1 + \alpha^2 L^2}} \right)^2. \quad (5)$$

Figure 3 shows examples for the PAR dependence of $\Phi_{\alpha\text{-pinene}}$, $\Phi_{\beta\text{-pinene}}$, and Φ_{acetone} . To allow comparison between calculated and measured emission rates, Φ_{VOC}^F was added again.

The solid lines are simulations using the results obtained from the fits. The PAR dependence of the acetone and α -pinene emissions is significant. The emission rates of β -pinene may be PAR-dependent. However, the error limits of Φ_{VOC}^B did not allow to quantify a possible PAR dependence. As expected, fits of the data measured for β -pinene and Δ^3 -carene led to results with large error limits.

Four measurement series were conducted to determine the

Table 1. Temperature Dependence of VOC Emissions From *Pinus sylvestris* As Obtained From Laboratory Experiments^a

| Acetone | Isoprene | α -pinene | Camphene | β -pinene | Δ^3 -carene | T Range, $^\circ\text{C}$ | PAR, $\mu\text{mol m}^{-2} \text{s}^{-1}$ |
|-------------------------|-------------------------|--------------------------|--------------------------|--------------------------|--------------------------|-----------------------------|-------------------------------------------|
| 4.6 ± 0.5 (0.79) | 5.3 ± 0.9 (0.8) | 11.1 ± 0.2 (0.97) | 10.8 ± 0.2 (0.95) | 10.3 ± 0.4 (0.95) | 11.9 ± 0.4 (0.96) | 13–29 | 0 |
| 4.7 ± 0.5 (0.81) | 7.7 ± 0.5 (0.92) | 10.8 ± 0.2 (0.99) | 10.8 ± 0.3 (0.97) | 11.0 ± 0.4 (0.98) | 11.8 ± 0.4 (0.97) | 17–33 | 360 |

^aData given in $[\text{K}] \times 10^{-3} \pm$ standard deviation (1σ). R^2 in brackets. For $\text{PAR} = 0$ the data represent c_{TP}/R (equation (2)).

Table 3. Temperature Dependence of Monoterpene Emissions From *Pinus sylvestris* Measured During Outdoor Experiments^a

| | Plant 1 June 8–11 9–36 | Plant 2 June 14–18 10–42 | Plant 3 July 6–7 12–39 | Plant 4 Aug. 26–27 14–40 |
|--------------------|------------------------------|--------------------------------|------------------------------|--------------------------------|
| <i>T</i> Range, °C | | | | |
| α -pinene | 7.1 \pm 0.6 (0.74) | 9.1 \pm 0.4 (0.91) | 6.0 \pm 1.2 (0.51) | 11.2 \pm 0.8 (0.88) |
| Camphene | 7.5 \pm 0.6 (0.76) | 9.4 \pm 0.5 (0.89) | 7.1 \pm 1.0 (0.68) | 10.2 \pm 1.0 (0.82) |
| β -pinene | 5.9 \pm 0.8 (0.56) | 9.7 \pm 0.5 (0.88) | 7.3 \pm 1.1 (0.65) | 11.7 \pm 0.9 (0.88) |
| Δ^3 -carene | 8.4 \pm 0.8 (0.72) | 11.9 \pm 0.4 (0.93) | 0.8 \pm 2.8 (0.004) | 13.8 \pm 0.9 (0.91) |

^aData given in [K] $\times 10^{-3} \pm$ standard deviation (1 σ). R^2 in brackets.

PAR dependence of VOC emission rates within a time period of 2 months. We found no significant differences for the data obtained for c_L and α . Hence we assume the mean of the data to be the best values. Table 4 summarizes the results.

At constant temperature the increase of the α -pinene and camphene emissions caused by PAR was between 20 and 30%. This increase was too low to be detected in the outdoor measurements. The relation between PAR and temperature at ambient conditions did not allow to find any PAR dependence.

4.4. Fits to the Complete Algorithm

One series of measurements to determine the PAR dependence of VOC emissions was conducted at different temperatures (23°, 27°, and 30°C, respectively). These measurements were made within a time period of 8 days, and temporal trends of the emission rates were assumed to be negligible on this timescale. This data set was fitted to the complete algorithm. For these fits the denominator in the last term of (3) was set to 1 since the experimental results showed no significant deviation from an exponential behavior up to temperatures even higher than 30°C. The fits were only conducted for acetone, isoprene, α -pinene, and camphene because no significant PAR

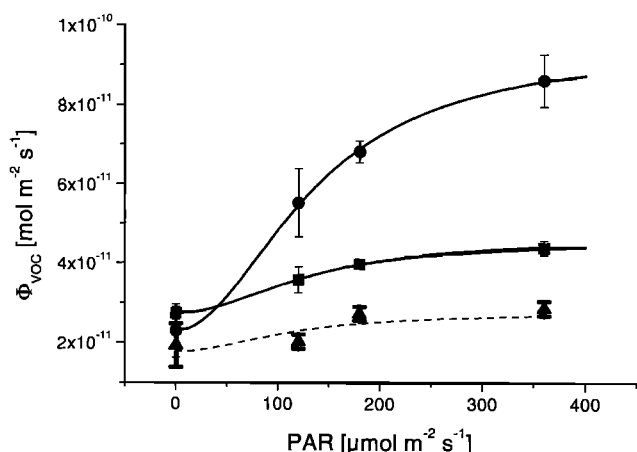


Figure 3. Plot of emission rates measured at a constant temperature of 27°C versus PAR. Squares: α -pinene, circles: acetone, triangles: β -pinene. Solid lines: simulations of the PAR dependence according to equation (5). Dashed line: best simulation for β -pinene.

Table 4. Mean Values for c_L and α^a

| | Acetone | Isoprene | α -pinene | Camphene |
|----------------------|-----------------|-----------------|------------------|-----------------|
| c_L | 1.08 \pm 0.05 | 1.15 \pm 0.06 | 1.1 \pm 0.14 | 0.98 \pm 0.05 |
| $\alpha \times 10^2$ | 0.8 \pm 0.17 | 0.75 \pm 0.29 | 0.98 \pm 0.62 | 1.43 \pm 0.67 |

^aGiven in [m² s μ mol⁻¹] $\times 10^2$. Data obtained from four measurement series in May and June. Errors are standard deviations (1 σ). For β -pinene and Δ^3 -carene a PAR dependence was not measurable ($\Phi_{VOC}^P \approx \Phi_{VOC}$).

dependence was found for the emission rates of β -pinene and Δ^3 -carene.

Table 5 shows the results obtained for the parameters c_{TP} , c_{T1} , c_L , and α together with standard emission rates. Within the error limits the results obtained for the individual parameters were consistent to those obtained from the other fits.

It should be noted that c_{TP}/R as determined for isoprene during that time period implied a decrease of $\Phi_{isoprene}^P$ with increasing temperature. This unusual behavior may result from a temporal trend of the isoprene darkness emissions. Such temporal trends may superimpose the temperature dependence of the emission rates.

4.5. Standard Emission Rates

The emission rates were normalized to 25°C and PAR equal to 1000 μ mol m⁻² s⁻¹ which are often used as standard conditions. For the plants investigated in the chamber experiments only those data were taken where PAR was above 300 μ mol m⁻² s⁻¹. Since Φ_{VOC}^P is PAR-saturated at that light level, a normalization procedure regarding the PAR dependence is not needed. For the plants investigated outdoors the emission rates were normalized to 25°C using the temperature dependence measured for the individual plants. Table 6 lists the standard emission rates for monoterpenes. These standard emission rates vary by up to an order of magnitude.

4.6. Labeling Experiment

In order to study the mechanisms responsible for VOC emissions from Scots pine in more detail, a single plant was exposed to ¹³CO₂. The plant was exposed to 320 ppm ¹³CO₂ (¹³C > 99%) at PAR equal to 800 μ mol m⁻² s⁻¹ and a temperature of 25°C. After 9 hours, at the end of the illumination period, ¹³CO₂ exposure was stopped, and the CSTR was flushed with air containing CO₂ with natural abundance of ¹³C.

Figure 4 shows the temporal behavior of isoprene emission rates and the ratio of isoprene labeled with at least one ¹³C atom to isoprene without labeling. Figure 5 shows the same for the emission rate of α -pinene, the labeling of its C₇ fragment, and the labeling of the C₇ fragment of Δ^3 -carene.

From Figure 4 it is obvious that the emitted isoprene molecules were labeled during ¹³CO₂ exposure. The emission rates of isoprene decreased after onset of darkness. Nevertheless, the emissions were still observable in darkness, and the labeling of isoprene during darkness stayed nearly constant.

Also, for α -pinene the labeling during ¹³CO₂ exposure was obvious. With the beginning of darkness the emission rate and the amount of labeling decreased for α -pinene. However, the labeling was significant also in darkness. Similar results were found for other monoterpenes such as β -pinene or Δ^3 -carene. The emission rates showed the same time shapes as those of α -pinene, both VOCs were also labeled, and the time shapes of labeling were similar to that of α -pinene (for labeling, see

Table 5. Data for $\Phi^{P,S}$ and $\Phi^{B,S}$ and Results From Fits to the Complete Algorithm^a

| | Acetone | Isoprene | α -pinene | Camphene |
|-------------------------------------------------------|-----------------|------------------|------------------|-----------------|
| $\Phi^{P,S} 10^{12}, \text{mol m}^{-2} \text{s}^{-1}$ | 23 ± 2 | 3 ± 1 | 26 ± 4 | 6 ± 0.4 |
| $\Phi^{B,S} 10^{12}, \text{mol m}^{-2} \text{s}^{-1}$ | 52 ± 7 | 6 ± 2 | 8 ± 2.3 | 4.1 ± 1.5 |
| $c_{TP}/R 10^{-3}, \text{K}$ | 3.2 ± 3.0 | -5.3 ± 3.5 | 12.5 ± 3 | 8.9 ± 3.1 |
| | (3.1 ± 0.3) | (-3.6 ± 0.7) | (9.4 ± 2.2) | (9.5 ± 0.8) |
| $c_{T1}/R 10^{-3}, \text{K}$ | 7.6 ± 2.4 | 7.3 ± 3.3 | 9.6 ± 2.5 | 8.9 ± 2.4 |
| | (9.2 ± 0.9) | (9.0 ± 1.3) | (11.4 ± 0.3) | (7.9 ± 2.0) |
| c_L | 0.7 ± 0.27 | 1.1 ± 0.3 | 1.6 ± 0.5 | 1.3 ± 0.2 |
| | (1.1 ± 0.1) | (1.2 ± 0.5) | (1.0 ± 0.2) | (1.0 ± 0.1) |
| $\alpha 10^2, \text{m}^2 \text{s} \mu\text{mol}^{-1}$ | 0.8 ± 0.17 | 0.3 ± 0.1 | 0.8 ± 0.3 | 1.1 ± 0.3 |
| | (0.7 ± 0.1) | (0.4 ± 0.2) | (1.0 ± 0.4) | (1.2 ± 0.3) |

^aFor comparison, the data obtained during the same measurement period but from fits to data sets measured at constant PAR or constant temperature, respectively, are given in parentheses.

Figure 5, Δ^3 -carene). The amount of labeling found for β -pinene and Δ^3 -carene was lower than that of α -pinene.

Labeling of the emitted VOCs occurred on a timescale of hours, and the increase of labeling with time was not linear. Some hours after starting the $^{13}\text{CO}_2$ exposure, effects of beginning saturation were observed, and even after 9 hours of $^{13}\text{CO}_2$ exposure, unlabeled VOCs were emitted. The mass spectra showed a bimodal distribution with one of the maxima being the mass of the unlabeled VOCs. The data obtained during $^{13}\text{CO}_2$ exposure (9 hours) were fitted to the following equation:

$$\frac{N^L}{N^U} = S \left(1 - \exp \left(-\frac{t}{\tau} \right) \right), \quad (6)$$

where N^L/N^U is the ratio of labeled molecules N^L to unlabeled molecules N^U as obtained from the mass spectra, t is the time (t in units of hours, $t = 0$ is the start of $^{13}\text{CO}_2$ exposure), and τ is the time required to incorporate a ^{13}C atom into the emitted VOC (here denominated as turnover time). S is the ratio for N^L/N^U that has to be expected for $t \gg \tau$ and reflects the amount of labeling at saturation. The results were $S = 0.9 \pm 0.06$; $\tau = 3 \pm 0.3$ (h) for isoprene, and $S = 0.4 \pm 0.08$; $\tau = 3.9 \pm 1.0$ (h) for α -pinene, respectively. The turnover time is about 3 to 4 hours. The amount of labeled molecules extrapolated to $t \gg \tau$ is about 50% for isoprene and about 30% for α -pinene, respectively.

Since the labeling occurred on a timescale of hours, we checked the temporal response of the emission rates with respect to changes of temperature or PAR. Measurements conducted under non-steady-state conditions were examined. Figure 6 shows the results from such a measurement. Changes of the emission rates caused by variations of temperature or PAR occurred on timescales shorter than the temporal resolution of our measurements (1/2 hour).

5. Discussion

The temperature dependencies determined for the monoterpene emissions are consistent with data given in literature (for a comparison between temperature coefficients given in units of K^{-1} (β), the data given here for c_{TP}/R have to be divided by $(298 \text{ K})^2$). Our results regarding the PAR dependence of α -pinene and camphene emissions seem to contradict many of those reported in literature.

One reason for this discrepancy is the early PAR saturation of these emissions occurring already at levels of about 15% of full sunlight. All measurements conducted above 15% of full sunlight will show no PAR dependence. Another reason is the small increase of monoterpene emissions caused by PAR. An increase of about 20 to 30% is not easily detectable especially for ambient studies where temperature and irradiation are correlated.

We started the measurements regarding the PAR dependence of the emission rates about a month after the plants were introduced into the chamber. The plants were held at a relatively low light intensity, and thus it cannot be excluded that the plants were shade-adapted. This may have led to the early PAR saturation. However, if the PAR dependence of monoterpene emissions would not be saturated at low PAR levels, the PAR dependence should be observable during the outdoor measurements. Hence we believe that the early PAR saturation as observed during our laboratory studies is not caused by a chamber artifact.

Moreover, the finding of the low PAR dependence is consistent with the labeling of these VOCs during $^{13}\text{CO}_2$ exposure which implies an influence of photosynthesis on the mechanism of monoterpene emissions. Also, β -pinene and Δ^3 -carene were labeled, but the amount of labeling was low. This can be expected if emissions in parallel with the biosynthesis of

Table 6. Standard Emission Rates ($\Phi_{\text{VOC}}^{P,S} + \Phi_{\text{VOC}}^{B,S}$)^a

| | Plant 1 June 8–11 | Plant 2 June 14–18 | Plant 3 July 6–7 | Plant 4 Aug. 26–27 | Indoor Plants May–June |
|--------------------|----------------------|-----------------------|---------------------|-----------------------|---------------------------|
| α -pinene | 7.8 ± 0.9 | 12.2 ± 0.7 | 87 ± 22 | 24 ± 2.4 | 37.2 ± 10.0 |
| Camphene | 4.4 ± 0.5 | 6.9 ± 0.5 | 9.3 ± 1.7 | 5.5 ± 0.7 | 10.5 ± 1.5 |
| β -pinene | 3.3 ± 0.6 | 2.4 ± 0.2 | 4.5 ± 0.9 | 12 ± 1.2 | 19.4 ± 2.0 |
| Δ^3 -carene | 11 ± 0.9 | 11 ± 0.6 | 0.2 ± 1.2 | 28 ± 2.5 | 24.2 ± 6.0 |

^aGiven in $[\text{mol m}^{-2} \text{s}^{-1}] \times 10^{12}$. The error in the emission rates given for the outdoor measurements are uncertainties from the fits to the data. Those given for the indoor measurements are standard deviations (1σ , measurement period 2 months).

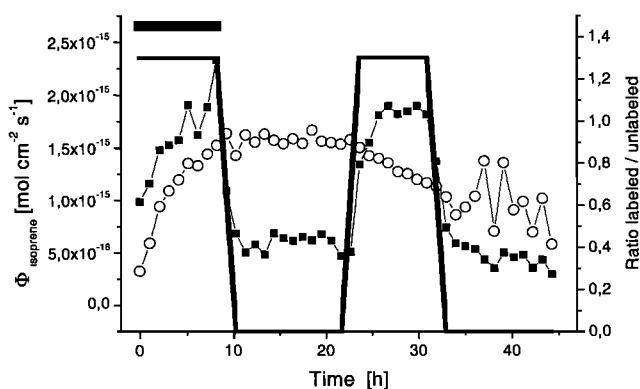


Figure 4. Temporal behavior of Φ_{isoprene} (solid squares, left scale) and labeling of isoprene (open circles, right scale). Solid line: PAR $800/0 \mu\text{mol m}^{-2} \text{s}^{-1}$. Bar: time of exposure to $^{13}\text{CO}_2$.

β -pinene and Δ^3 -carene are small compared to those from pools. Thus it is not surprising that the PAR dependence of the emission rates of these compounds was not detectable within the accuracy of our measurements.

The temperature and PAR dependence of VOC emissions from *Pinus sylvestris* can be described with the algorithm of Schuh *et al.* [1997]. By the assumption of two independent emission processes it is possible to consider nighttime emissions as well as a PAR dependence of emissions. To describe VOC emissions from Scots pine exactly, an algorithm of this type is needed. Only in special cases the contributions of Φ_{VOC}^P or Φ_{VOC}^B , respectively, are negligible and the algorithms may be simplified.

However, models regarding the mechanisms of VOC emissions have to be changed. The results of our labeling experiment imply (1) biosynthesis of monoterpenes in darkness, (2) synthesis within different biosynthetic pathways, and (3) large pools for precursors of isoprene and monoterpenes.

1. No pools are known for isoprene. Considering the high vapor pressure of isoprene (750 mbar at 25°C) it seems highly improbable that there are storage pools for isoprene in the needles of *Pinus sylvestris*. Therefore we assume that the release of isoprene during darkness occurs either in parallel with

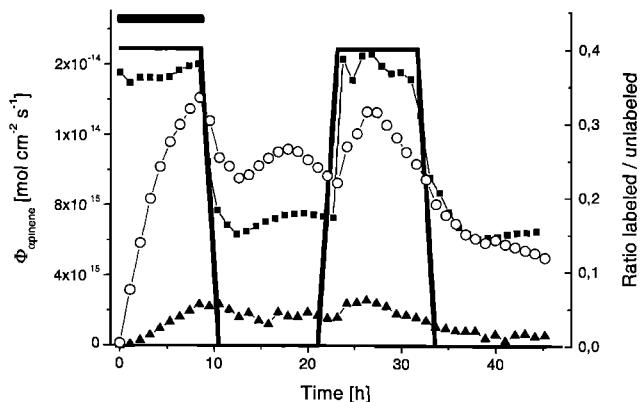


Figure 5. Temporal behavior of $\Phi_{\alpha\text{-pinene}}$ (solid squares), labeling of the C_7 fragment of α -pinene (open circles), and labeling of the C_7 fragment of Δ^3 -carene (triangles). Solid line: PAR ($800/0 \mu\text{mol m}^{-2} \text{s}^{-1}$). Bar: duration of $^{13}\text{CO}_2$ exposure.

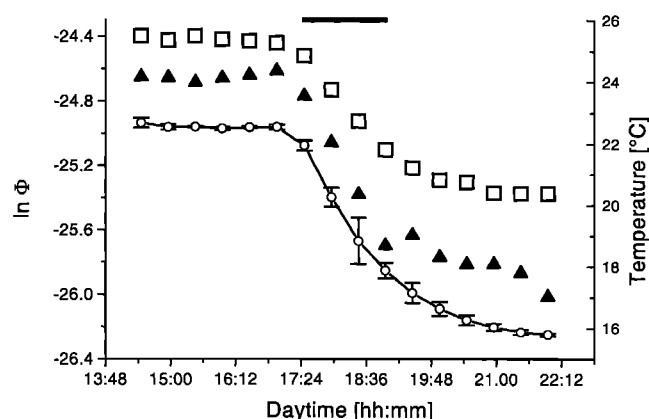


Figure 6. Temporal behavior of isoprene and α -pinene emission rates during twilight. Open squares: $\ln(\Phi_{\alpha\text{-pinene}})$, left scale. Triangles: $\ln(\Phi_{\text{isoprene}})$ (multiplied by 2.5). Open circles: temperature, right scale the error bars indicate the range of temperature during the sampling period. The bar indicates duration of twilight.

isoprene biosynthesis or as a non enzymatic breakdown of the precursor of isoprene, dimethyl-allyl-pyrophosphate (DMAPP). We cannot distinguish between these two different ways. However, the labeling of isoprene during darkness shows clearly that isoprene must have been produced from the carbon taken up during $^{13}\text{CO}_2$ exposure.

As can be seen from Figure 5, also α -pinene is labeled during darkness. This cannot be explained if it is exclusively emitted from storage pools. Also monoterpenes must have been produced from CO_2 taken up recently. But there are differences between the labeling of α -pinene and isoprene: The amount of α -pinene labeling is lower than that of isoprene and the labeling of α -pinene decreases after onset of darkness.

The most probable explanation for these differences is that α -pinene is emitted from pools as well as in parallel with α -pinene biosynthesis. Emissions linked to α -pinene synthesis are PAR dependent and therefore lower in darkness than under illumination. $\Phi_{\alpha\text{-pinene}}^B / \Phi_{\alpha\text{-pinene}}^P$ decreases with decreasing illumination which leads to the lower labeling during the dark phase. However, α -pinene synthesis during darkness is not zero. Our results indicate that a substantial part of the α -pinene emitted during darkness must have been synthesized from the carbon taken up during $^{13}\text{CO}_2$ exposure. Monoterpenes are synthesized in *Pinus sylvestris* also during darkness.

2. The results of our labeling experiment imply that biosynthetic VOC production in *Pinus sylvestris* occurs within two different pathways. The saturation effects observed for the labeling of isoprene (Figure 4) cannot be explained by emissions of isoprene from storage pools in parallel with the emissions linked to isoprene synthesis. This saturation can easily be explained by the 2 known different pathways for the production of DMAPP [Lichtenthaler, 1999]. DMAPP, the precursor of isoprene, can be produced via two independent pathways. The turnover time from the CO_2 taken up to the emitted isoprene may be different for these different pathways. If the turnover in one of these pathways is slow compared to the duration of $^{13}\text{CO}_2$ exposure, a saturation of labeling at levels below 100% has to be expected. Our results imply that isoprene is produced in *Pinus sylvestris* by about 50% via both pathways.

DMAPP is also a precursor of monoterpenes and therefore also monoterpenes may be produced by these different pathways. However, our results do not allow to examine relative amounts of monoterpene synthesis within these pathways. The saturation effects of monoterpene labeling can indicate both, emissions from large storage pools as well as a long turnover time from the CO₂ taken up to the emitted monoterpene in one of the pathways producing DMAPP.

3. Besides the saturation effects the temporal behavior of labeling has to be discussed. The temporal shape of the labeling may be determined by the turnover time of the ¹³C atoms within both pathways that produce DMAPP. However, the saturation of isoprene labeling implies that the turnover of carbon within one of these pathway is much longer than the exposure time of 9 hours. Thus the temporal increase of labeling reflects mainly the turnover in the pathway with the shorter turnover time for carbon.

This turnover time is in the range of several hours which is much longer than those reported in literature. For example, Sharkey *et al.* [1991] show a labeling of isoprene occurring on a time scale of minutes. From this finding they conclude that leaves of red oak have only a small pool of isoprene precursors and furthermore, that isoprene emissions follow isoprene biosynthesis nearly directly. However, the long turnover time resulting from our measurements does not contradict our assumption that Φ_{VOC}^B follows biosynthesis on a short timescale.

We assume that a major rate limiting step for the turnover is in one of the precursor reactions before DMAPP biosynthesis. Although the turnover time to the emitted α -pinene seems to be somewhat longer than that to isoprene, these turnover times are similar. This similarity implies a major rate-limiting step common for both compounds. Since DMAPP is the last common precursor of both VOCs the carbon turnover should be limited by reactions before DMAPP synthesis. If so, the turnover time may be long but the VOC emissions can follow biosynthesis of the individual compounds very quickly. The fast response of the emission rates to changes of temperature or PAR (see Figure 6) supports this assumption. Because biosynthetic activity itself is related to temperature and PAR, both variables can be used to describe the emission rates.

In summary, the mechanisms of VOC emissions from *Pinus sylvestris* are more complex than previously thought. Isoprene synthesis and subsequent emissions are due to 2 different biosynthetic pathways. Monoterpene emissions are caused by emissions from pools as well as by processes linked to monoterpene biosynthesis. Emissions linked to VOC synthesis occur during illumination as well as during darkness.

Nevertheless, the algorithm of Schuh *et al.* [1997] describes the temperature and PAR dependence of VOC emissions from *Pinus sylvestris* quite well. The detailed mechanisms of VOC emissions are simplified into a light-dependent and a light-independent process. Temperature and PAR are the only variables used to describe the emission rates.

The light-independent process only depends on temperature. To describe the temperature dependence, it is unnecessary to distinguish between emissions from pools and from processes linked to VOC biosynthesis. The net effect of temperature on Φ_{VOC}^B is described by the algorithm independent of the mechanisms leading to VOC emissions during darkness. Furthermore, it seems unnecessary to distinguish between different biochemical pathways that produce the VOCs. These different mechanisms might have different temperature or

PAR dependencies but again, a description just needs to consider the net effects of temperature and PAR on Φ_{VOC}^B .

On the one hand, the algorithm of Schuh *et al.* [1997] allows an exact description without needing to consider the detailed mechanisms of VOC emissions. On the other hand, the mechanisms of VOC emissions allow isoprene emissions during darkness and a PAR dependence of monoterpene emissions. The more detailed insight into the mechanisms of VOC emissions obtained from our labeling experiments shows clearly that algorithms have to describe both, a PAR dependence of VOC emissions as well as emissions during darkness.

The algorithm of Schuh *et al.* [1997] allows to describe the influence of temperature and PAR on VOC emissions. However, VOC emissions are also affected by other factors than temperature and PAR. Up to now the dependence of VOC emissions on other factors is included in the standard emission rates that are used as normalization factors. These standard emission rates have to be determined experimentally and they vary from plant to plant (see Table 6). Obviously, other factors can cause a variability of emission rates by an order of magnitude but their influence on the emission rates is not described yet. More knowledge about the mechanisms controlling the VOC emissions from plants is required to allow a reliable description of the emission rates.

6. Summary

We found that monoterpene emissions from *Pinus sylvestris* are affected by temperature and PAR. Temperature is the most important factor affecting monoterpene emissions. However, to describe monoterpene emissions exactly, the influence of PAR has to be considered. Furthermore, we observed isoprene emission from *Pinus sylvestris* in darkness. Our results show that also these darkness emissions have to be considered to describe the isoprene emissions.

From the results of labeling experiments we obtained more knowledge about the mechanisms of VOC emissions. Isoprene emissions in parallel with isoprene synthesis occurs during illumination as well as in darkness. Also, monoterpenes are emitted by mechanisms linked to their synthesis during illumination and during darkness. These mechanisms of VOC emissions imply that some commonly used algorithms describing isoprene or monoterpene emissions have to be extended. The algorithm given by Schuh *et al.* [1997] is suitable to describe the influence of temperature and PAR on isoprene and monoterpene emissions from *Pinus sylvestris*. Also, the acetone emissions can be described quite well.

Acknowledgments. This work was financially supported by the Bundesministerium für Bildung, Wissenschaft, Forschung und Technologie within the Tropospheric Research Programme under grants 07TFS23 and 07TFS24. M.S. thanks the scholarship provided by Forschungszentrum Jülich and the training program UNDP. J.W. would like to acknowledge financial assistance by the Fonds der Chemischen Industrie.

References

- Dement, W., B. Tyson, and H. Mooney, Mechanism of monoterpene volatilization in *Salvia mellifera*, *Phytochemistry*, **14**, 2555–2557, 1975.
- Gautrois, M., and R. Koppmann, Diffusion technique for the production of gas standards for atmospheric measurements, *J. Chromatogr. A*, **848**, 239–249, 1999.
- Goldan, P. D., W. C. Kuster, and F. C. Fehsenfeld, Hydrocarbon

- measurements in the southeastern United States: The Rural Oxidants in the Southern Environment (ROSE) program, *J. Geophys. Res.*, **100**, 25,945–25,963, 1995.
- Guenther, A. B., P. R. Zimmerman, P. C. Harley, R. K. Monson, and R. Fall, Isoprene and monoterpene emission rate variability: Model evaluations and sensitivity analyses, *J. Geophys. Res.*, **98**, 12,609–12,617, 1993.
- Guenther, A., et al., A global model of natural volatile organic compound emissions, *J. Geophys. Res.*, **100**, 8873–8892, 1995.
- Heiden, A. C., et al., Emission of volatile organic compounds from ozone-exposed plants, *Ecol. Appl.*, **9**, 1160–1167, 1999.
- Janson, R. W., Monoterpene emissions from Scots pine and Norwegian spruce, *J. Geophys. Res.*, **98**, 2839–2850, 1993.
- Juuti, S., J. Arey, and R. Atkinson, Monoterpene emission rate measurements from a Monterey pine, *J. Geophys. Res.*, **95**, 7515–7519, 1990.
- Komenda, M., E. Parusel, A. Wedel, and R. Koppmann, Measurements of biogenic VOC emissions: Sampling, analysis and calibration, *Atmos. Environ.*, **35**, 2069–2080, 2001.
- Lamb, B., H. Westberg, G. Allwine, and T. Quarles, Biogenic hydrocarbon emissions from deciduous and coniferous trees in the United States, *J. Geophys. Res.*, **90**, 2380–2390, 1985.
- Lamb, B., A. Guenther, D. Gay, and H. Westberg, A national inventory of biogenic hydrocarbon emissions, *Atmos. Environ.*, **21**, 1695–1705, 1987.
- Lerdau, M., Plant function and biogenic terpene emission, in *Trace Gas Emissions by Plants*, edited by T. D. Sharkey, E. A. Holland, and H. A. Mooney, pp. 93–119, Academic, San Diego, Calif., 1991.
- Lichtenthaler, H., The 1-deoxy-D-xylulose-5-phosphate pathway of isoprenoid biosynthesis in plants, *Ann. Rev. Plant Physiol. Plant Mol. Biol.*, **50**, 47–65, 1999.
- Loreto, F., and T. D. Sharkey, On the relationship between isoprene emission and photosynthetic metabolites under different environmental conditions, *Planta*, **189**, 420–424, 1993.
- Peterer, J., and C. Körner, Das Problem der Bezugsgröße bei physiologisch-ökologischen Untersuchungen an Koniferennadeln, *Forstw. Cbl.*, **109**, 220–241, 1990.
- Rasmussen, R. A., What do trees contribute to air pollution?, *J. Air Pollut. Control Assoc.*, **2**, 537–543, 1972.
- Schuermann, W., H. Ziegler, D. Kotzias, R. Schoenwitz, and R. Steinbrecher, Emission of biosynthesized monoterpenes from needles of Norway Spruce, *Naturwissenschaften*, **80**, 276–278, 1993.
- Schuh, G., A. C. Heiden, T. Hoffmann, J. Kahl, P. Rockel, J. Rudolph, and J. Wildt, Emission of volatile organic compounds from sunflower and beech: Dependence on temperature and light intensity, *J. Atmos. Chem.*, **27**, 291–318, 1997.
- Sharkey, D. T., F. Loreto, and C. F. Delwiche, The biochemistry of isoprene emission from leaves during photosynthesis, in *Trace Gas Emissions by Plants*, edited by T. D. Sharkey, E. A. Holland, and H. A. Mooney, pp. 153–184, Academic, San Diego, Calif., 1991.
- Simon, V., B. Clement, M. L. Riba, and L. Torres, The Landes experiment: Monoterpenes emitted from the maritime pine, *J. Geophys. Res.*, **99**, 16,501–16,510, 1994.
- Simpson, D., A. B. Guenther, C. N. Hewitt, and R. Steinbrecher, Biogenic emissions in Europe, 1, Estimates and uncertainties, *J. Geophys. Res.*, **100**, 22,875–22,890, 1995.
- Simpson, D., et al., Inventorying emissions from nature in Europe, *J. Geophys. Res.*, **104**, 8113–8152, 1999.
- Street, R. A., S. C. Duckham, and C. N. Hewitt, Laboratory and field studies of biogenic volatile organic compound emissions from Sitka spruce (*Picea sitchensis* Bong.) in the United Kingdom, *J. Geophys. Res.*, **101**, 22,799–22,806, 1996.
- Tingey, D. T., M. Manning, L. C. Grothaus, and W. F. Burns, Influence of light and temperature on monoterpene emission rates from slash pine, *Plant Physiol.*, **65**, 797–801, 1980.
- Tingey, D. T., D. P. Turner, and J. A. Weber, Factors controlling the emissions of monoterpenes and other volatile organic compounds, in *Trace Gas Emissions by Plants*, edited by T. D. Sharkey, E. A. Holland, and H. A. Mooney, pp. 93–119, Academic, San Diego, Calif., 1991.
- Wedel, A., K. P. Müller, M. Ratte, and J. Rudolph, Measurements of volatile organic compounds (VOC) during POPCORN 1994: Applying a new on-line GC-MS technique, *J. Atmos. Chem.*, **31**, 73–103, 1998.
- Wildt, J., D. Kley, A. Rockel, P. Rockel, and H. J. Segschneider, Emission of NO from several higher plant species, *J. Geophys. Res.*, **102**, 5919–5927, 1997.
- K. V. Czapiewski, Center for Atmospheric Chemistry, York University, 4700 Keele St., Toronto, Ontario, Canada M3J 1P3.
- A. C. Heiden, Gerstel GmbH & Co. KG, Aktienstr. 232-234, D-45473 Mülheim/Ruhr, Germany.
- K. Kobel and J. Wildt (corresponding author), Institut für Chemie der Belasteten Atmosphäre, Forschungszentrum Jülich, 52425 Jülich, Germany. (j.wildt@fz-juelich.de)
- M. Komenda and R. Koppmann, Institut für Chemie und Dynamik der Geosphäre II: Troposphäre, Forschungszentrum Jülich, 52425 Jülich, Germany.
- M. Shao, State Key Laboratory of Environmental Simulation and Pollution Control, Peking University, No. 5, Yiheyuan Road, Haidian District, 100871 Beijing, China.

(Received December 11, 2000; revised March 28, 2001; accepted April 27, 2001.)